

Many-body localized phase of bosonic dipoles in a tilted optical lattice

Anirban Dutta¹, Subroto Mukerjee², and K. Sengupta³

¹*Centre for High Energy Physics, Indian Institute of Science, Bengaluru 560012, India*

²*Department of Physics, Indian Institute of Science, Bengaluru 560012, India*

³*Theoretical Physics Department, Indian Association for the Cultivation of Science, Jadavpur, Kolkata 700032, India*

(Dated: July 20, 2021)

We chart out the ground state phase diagram and demonstrate the presence of a many-body localized (MBL) phase for an experimentally realizable one-dimensional (1D) constrained dipole boson model in the presence of an Aubry-Andre (AA) potential whose strength λ_0 can be tuned to precipitate an ergodic-MBL transition. We discuss the signature of such a transition in the quantum dynamics of the model by computing its response subsequent to a sudden quench of λ_0 . We show that the MBL and the ergodic phases can be clearly distinguished by study of post-quench dynamics and provide an estimate for minimal time up to which experiments need to track the response of the system to confirm the onset of the MBL phase. We suggest experiments which can test our theory.

Ultracold bosonic atoms in an optical lattice form one of the most experimentally and theoretically well-studied strongly correlated systems in recent times^{1–5}. The central interest in these systems initially stemmed from the experimental demonstration of the existence of a quantum phase transition (QPT) of the constituent bosons from a superfluid to a Mott insulating (MI) phase⁶. It was later realized that in the presence of an effective electric field (or equivalently in a tilted optical lattice), the bosons, in their MI state, undergo yet another QPT which belongs to the Ising universality class⁷. Such an electric field can be generated either by shifting the center of the trap used to confine the atoms¹ or by applying a linearly varying Zeeman field⁶. This transition takes the system from a parent MI state with n_0 bosons per site to a Z_2 symmetry broken state with $n_0 \pm 1$ bosons occupying every alternate site. The physics of the transition and the phases separated by it is conveniently described in terms of dipoles, which are bound states of bosons and holes in adjacent sites as shown in Fig. 17. The physics of these systems for $d > 1$ ^{7,8} and their non-equilibrium dynamics for $d = 1$ has also been studied^{9,10}. The latter works^{9,10} indicated that such systems can act as test beds for a realization of the Kibble-Zurek mechanism. Furthermore, such constrained dipole models with additional density-density interaction between bosons realize Z_3 and Z_4 symmetry broken phases¹¹; these models have recently been experimentally realized using a Rydberg atom chain¹².

Many-Body Localization (MBL) in interacting quantum systems is one of the most widely studied phenomena in recent times^{13,14}. The loss of ergodicity in such systems due to strong disorder or quasiperiodic potentials has been confirmed theoretically by a wide variety of numerical and semi-analytic studies^{15,16}. The observation of MBL requires a high degree of isolation of the experimental system from the environment, rendering systems of cold atoms and ions as ideal testbeds. However, only

a few such systems are currently available^{17,18}. Thus, identification of other, currently realizable, experimental systems which may display MBL phases is of central importance to the field.

In this work, we show that the constrained dipole model realized experimentally in Ref. 6, in the presence of an additional Aubry-Andre (AA) potential, supports an ergodic-MBL transition (for the properties of the model in the presence of on-site disorder, see Ref. 19). The Hamiltonian of this constrained dipole model can be described in terms of dipole creation operator d_ℓ^\dagger on a link ℓ between two sites i and j of the 1D lattice⁷. These operators are related to the creation (b_j^\dagger) and annihilation (b_i) operators of the original bosons: $d_i^\dagger = b_i b_j^\dagger / \sqrt{n_0(n_0 + 1)}$. We analyze this dipole Hamiltonian by carrying out exact diagonalization (ED) on finite-size boson chains with $L \leq 18$ to obtain our main results which are as follows.

First, we compute the ratio of the difference of successive gaps in the energy spectrum and the entanglement entropy, both of which can be measured experimentally^{17,18}. In addition, we compute the Normalized Participation Ratio (NPR)¹⁵. The behavior of all these quantities demonstrate the existence of localized and ergodic phases in our model and a transition between them. Second, we chart out the long-time behavior of the dipole order parameter in the Z_n symmetry broken phase (Fig. 1) where there is one dipole every n sites, $O_d^{(n)} = \sum_\ell d_\ell^\dagger d_\ell \cos(2\pi\ell/n)/L$, for $n = 3$ following a sudden quench of the AA potential. The post-quench dynamics indicates thermalization (or lack thereof) of $O_d^{(3)}$ in the ergodic (MBL) phase leading to its qualitatively distinct behavior at long times in these two phases. Third, we provide an estimate of the minimum time up to which the experiments need to track the behavior of $O_d^{(3)}(t)$ to ascertain the onset of the MBL phase. We note that such qualitatively distinct nature of $O_d^{(3)}(t)$ can be experimentally detected via parity of oc-

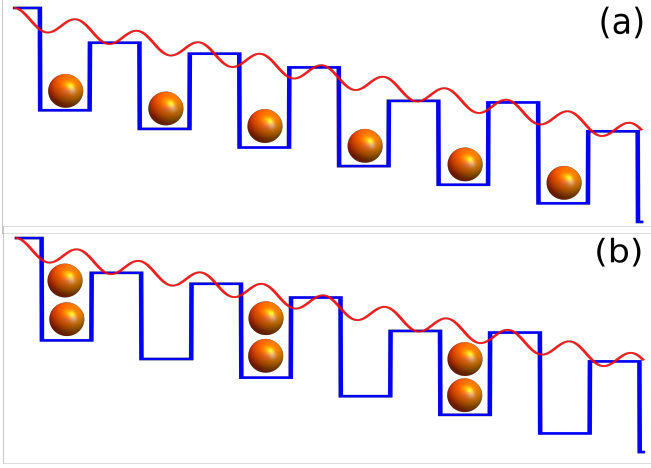


FIG. 1: (a) A schematic representation of the parent Mott state of the tilted Bose-Hubbard model in the presence of the AA potential. (b) A schematic representation of a Z_2 symmetry broken dipole ordered state¹⁹.

cupation measurement^{6,12}. This feature allows one to obtain an unambiguous signature of the MBL phase within experimentally relevant time scales. We also note that the Hamiltonian we study has a truncated Hilbert space arising from the constraint of not allowing dipoles to occupy adjacent sites, as will be explained later. Our study therefore demonstrates that MBL can occur in systems with truncated Hilbert spaces.

We begin by specifying the 1D boson Hamiltonian in an optical lattice in the presence of an AA potential which is given by

$$H_B = -J \sum_{\langle ij \rangle} b_i^\dagger b_j + \sum_j \left[\frac{U}{2} n_j(n_j - 1) + (\lambda_j - \mathcal{E}j)n_j \right]$$

where $\lambda_j = \lambda_0 \cos(2\pi\beta j + \phi)$ is the AA potential, $\beta = 2/(\sqrt{5} - 1)$ is the golden ratio conjugate, \mathcal{E} is the effective electric field^{1,6}, U is the on-site interaction between the bosons, J is the hopping potential, ϕ is the offset angle, and $\langle ij \rangle$ indicates that j is one of the neighboring sites of i . In the absence of λ_j and in the regime $U, \mathcal{E} \gg |U - \mathcal{E}|, J, \lambda_0$, the low-energy physics of this systems can be described in terms of dipole operators since these excitations are resonantly connected to the parent Mott state⁷. The on-site energy for formation of these dipoles is $\mu_d = U - \mathcal{E}$ (see Fig. 1) and the hopping term J allows for spontaneous creation and annihilation of these dipoles leading to non-conservation of dipole number.

In the presence of the AA potential, the on-site energy cost for creation of dipoles is modified. The bosons feel a difference in potential originating from the AA term when it hops to the neighboring site. A straightforward

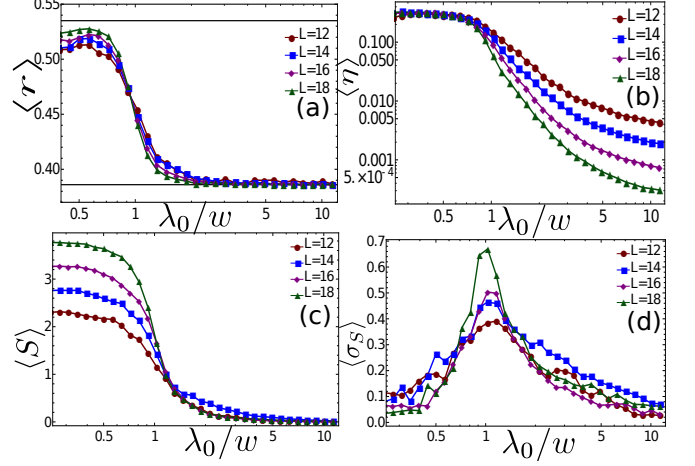


FIG. 2: (a) Plot of $\langle r \rangle$ as a function of λ_0 showing an ergodic-MBL transition at $\lambda_0/w \simeq 0.946$. (b) A plot of NPR, η as a function of λ_0 for several L . (c) Plot of the half-chain entanglement entropy S as a function of λ_0 . (d) Plot of fluctuation of entanglement, σ_s , as a function of λ_0 . For all plots, $U_0 - \mathcal{E}/w = 0$.

calculation yields

$$\mu_d(\ell) = U - \mathcal{E} + V'_0 \cos(2\pi\beta\ell - \phi_0 + \phi) \quad (1)$$

where $V'_0 = -2\lambda_0 \sin(\pi\beta)$ and $\phi_0 = \pi/2$, and ϕ may be used to produce different realizations of this quasiperiodic potential. Thus the dipoles see an effective AA potential with modified amplitude which can be controlled by tuning λ_0 . Moreover, as long we restrict ourselves to the regime $U, \mathcal{E} \gg |U - \mathcal{E}|, J, \lambda_0$, states with two dipoles on a given link or on two consecutive links do not form a part of the low-energy subspace⁷. Thus the effective dipole model describing the low-energy physics of the model can be written as⁷

$$H_d = \sum_{\ell} (-w(d_{\ell}^\dagger + d_{\ell}) + \mu_d(\ell)\hat{n}_{\ell}^d) \quad (2)$$

$$n_{\ell}^d \leq 1, \quad n_{\ell}^d n_{\ell+1}^d = 0$$

where $\hat{n}_{\ell}^d = d_{\ell}^\dagger d_{\ell}$ is the dipole number operator and $w = J\sqrt{n_0(n_0 + 1)}$. The constraints $n_{\ell}^d \leq 1$ and $n_{\ell}^d n_{\ell+1}^d = 0$ truncate the size of the Hilbert space by eliminating states with dipoles on adjacent sites. The ground state phase diagram of the model, which contains a Z_2 symmetry broken phase as shown in Fig. 1(b), is charted out in the supplemental information¹⁹.

We now focus on the ergodic-MBL transition in this model. At the outset, we note that a MBL phase of the dipole model (Eq. 2) does not amount to that of the original boson model (Eq. 1) since the latter has additional states which are not part of the former's Hilbert

space. However, we expect experiments discussed in Ref. 12 (which emulates H_d (Eq. 2) using a Rydberg atom chain) to exhibit the MBL phase of H_d . We shall discuss this point later in details. To study the MBL phase and the associated ergodic-MBL transition, we fix \mathcal{E} and obtain the eigenvalues and eigenvectors of the model for $L \leq 18$ using ED for several values of λ_0 . We then use these to compute three quantities which may distinguish between ergodic and MBL phases.

The first of these is the ratio of the difference of successive gaps in the energy spectrum, $r_n = \text{Min}[\Delta_{n+1} - \Delta_n] / \text{Max}[\Delta_{n+1} - \Delta_n]$, where $\Delta_n = E_{n+1} - E_n$, and E_n denotes the eigenvalues of H_d . It is well known that r_n obeys Poisson (GOE) statistic in the MBL (ergodic) phase with the mean value $\langle r \rangle = 0.386(0.535)^{13,14}$. The second, is the NPR defined as $\eta = \sum_n |\psi_n|^4 / \mathcal{D}$, where $\psi_n = \langle n | \psi \rangle$, $|\psi\rangle$ is the wavefunction of a typical state with finite energy density, and $|n\rangle$ denotes eigenstates of \hat{n}_d . η is expected to be a system-size independent constant in the ergodic phase; in contrast, it decays exponentially with system size in the MBL phase¹⁵. Finally, we compute the entanglement entropy $S = -\text{Tr} \rho \ln \rho$ for a given subsystem of length $L/2$ described by a density matrix ρ for a representative state with finite energy density in the middle of the spectrum. For such a typical state, S follows a volume(area) law in the ergodic(MBL) phase^{13,14}. In addition, we also compute the fluctuation of the entanglement entropy, σ_S , as a function of λ_0 . Each of these quantities, as we find below, provides an independent measure to discern between ergodic and MBL phases.

The results obtained from these calculations are shown in Fig. 2 which indicate a finite-size crossover from ergodic to MBL phase around $\lambda_0 \simeq w$. Fig. 2(a) shows that $\langle r \rangle$ changes from its expected values in the ergodic phase to that in the MBL phase around $\lambda_{0c} \simeq 0.95w$ where curves corresponding to different L s cross. A similar trend is noticed in Fig. 2(b) where η becomes L dependent around λ_{0c} indicating the onset of a MBL phase. In Fig. 2(c), we find that S becomes independent of system size for $\lambda_0 > \lambda'_{0c} \simeq 1.25w$ indicating an area law behavior for a generic state in the middle of the spectrum and therefore a MBL phase. Finally, in Fig. 2(d), we find enhancement of σ_s around λ'_{0c} indicating presence of strong quantum fluctuation at this point. Thus our data establishes the presence of a MBL phase in the constrained dipole boson model. Note that the critical λ_0 from the two diagnostics ($\langle r \rangle$ and S) do not in general agree exactly for system sizes accessible to ED²⁰.

The experimental signature of such a MBL phase is most easily picked up in dynamics. To this end, we study the behavior of the dipole order parameter in the Z_3 symmetry broken ground state, $\langle O_d^{(3)} \rangle(t)$, as a function of time following a sudden quench of λ_0 (for behavior of S following such a quench see Ref. 19). We

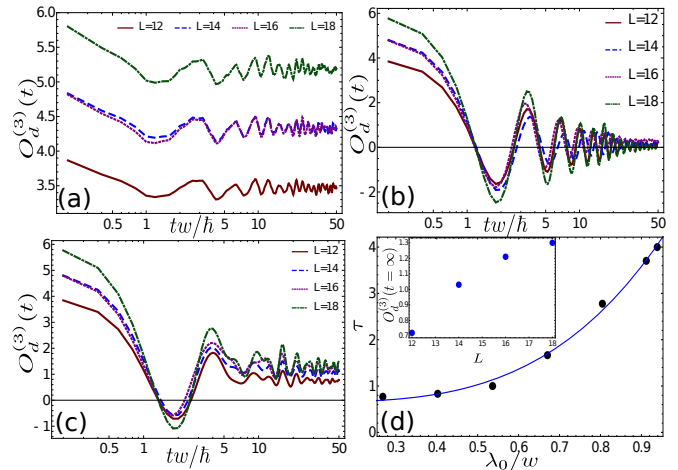


FIG. 3: (a) Plot of $\langle O_d^{(3)} \rangle(t)$ as a function of time in the MBL phase with $\lambda_0/w = 5.37$. (b) Same as in (a) but in the ergodic phase with $\lambda_0/w = 0.268$. (c) Same as in (a) at $\lambda_{0c} = 0.95w$. (d) Plot of the decay time τ of the oscillations of $O_d^{(3)}(t)$ as a function of λ/w . The inset shows the L dependence of $O_d^{(3)}(t \rightarrow \infty)$ at λ_{0c} . See text for details.

start from the Z_3 symmetry-broken dipole-ordered state $|\psi_0(t=0)\rangle$, (which is a ground state of H_{Ryd} as discussed above), and perform a sudden quench of $V_{jj'}$, λ_0 with $\Delta \equiv (U - \mathcal{E}_0)/w = 5$ so that the final Hamiltonian has a Z_2 symmetry broken ground state. One can then write $|\psi(t)\rangle = \sum_{c_m} \exp[-iE_m t/\hbar] |m\rangle$, $|m\rangle$ and E_m denote the eigenstates and eigenvalues of the new Hamiltonian and $c_m = \langle m | \psi_0(t=0) \rangle$. Using this one obtains

$$\langle O_d^{(3)} \rangle(t) = \sum_{m,n} c_m^* c_n e^{-i(E_n - E_m)t/\hbar} \langle m | O_d^{(3)} | n \rangle. \quad (3)$$

A plot of $\langle O_d^{(3)} \rangle(t)$ as a function of time, shown in Fig. 3(a) clearly shows that in the MBL phase where $\lambda_0 \gg \lambda_{0c}$, $\langle O_d^{(3)} \rangle(t)$ remains finite over a long period of time. In contrast, as shown in Fig. 3(b), in the ergodic phase where $\lambda_0 \ll \lambda_{0c}$, it decays to zero over a short time scale after a few oscillations. At $\lambda_0 = \lambda_{0c}$, as shown in Fig. 3(c), $\langle O_d^{(3)} \rangle(t)$ oscillates initially but decays to a final value which approaches zero for $L \rightarrow \infty$ as shown in the inset of Fig. 3(d). The decay time τ of $O_d^{(3)}(t)$ is obtained by fitting its oscillation envelope to $A \exp[-t/\tau]$ where A and τ are fitting parameters. In the ergodic phase, as shown in Fig. 3(d), τ increases with λ with $\tau w/\hbar \simeq 4$ for $\lambda = 0.94$; it diverges in the MBL phase.

The most suitable platform for experimental realization of our work constitutes an array of Rydberg atoms. These systems, in the absence of AA potential, have recently been realized experimentally in Ref. 12. The

Hamiltonian of these Rydberg atoms is given by

$$H_{\text{Ryd}} = \sum_j (-\Omega \sigma_j^x + \Delta_0 \hat{n}_j) + \sum_{jj'} V_{jj'} \hat{n}_j \hat{n}_{j'} \quad (4)$$

where \hat{n}_j denotes the number operator for Rydberg (excited) atoms on site j , Δ_0 denotes detuning parameter which can be used to excite an atom to a Rydberg state, $V_{jj'} \sim 1/|x_j - x_{j'}|^6$ denotes the interaction strength between two Rydberg atoms and $\sigma_j^x = |r_j\rangle\langle g_j| + |g_j\rangle\langle r_j|$ denotes the coupling between the Rydberg ($|r_j\rangle$) and ground ($|g_j\rangle$) states. We note that for $V_{jj'} = 0$, Eq. 4 can be directly mapped to Eq. 2 via the identification $\Omega \rightarrow w$, $\Delta_0 \rightarrow \mu_d$ and $\hat{n}_j \rightarrow \hat{n}_d$. In experiments, $V_{jj'}$ could be tuned so that $V_{j,j+1} \gg \Delta_0, \Omega$ and $V_{j,j+n} \ll \Delta_0, \Omega$ for $n > 1$. This effectively implements the constraint $\hat{n}_\ell^d \hat{n}_{\ell+1}^d = 0$ leading to realization of H_d with Z_2 symmetry broken ground state for $\Delta_0 \ll 0^{12}$. Other configurations of $V_{jj'}$ where $V_{j,j+n} \gg \Delta_0, \Omega$ for $n = 1, 2$ led to experimental realization of the Z_3 states. Such a state turns out to also be the ground state of H_d supplemented with an additional dipole-dipole interaction term^{11,21}. We also note that there have been concrete proposals for realization of the AA potential for ultracold atom chains²². In what follows, we propose that such potentials are applied on the Rydberg atom chain studied in Ref. 12.

The dynamics of $\langle O_d^{(3)} \rangle(t)$ can be studied experimentally by first preparing a Rydberg chain in a ground state of H_{Ryd} with $V_{j,j+n} \gg \Delta_0, \Omega$ for $n = 1, 2$ and $\lambda_0 = 0$. This is to be followed by sudden quenches of $V_{jj'}$ and λ_0 such that $V_{j,j+n} \gg \Delta_0, \Omega$ for $n = 1$ and λ_0 has a desired finite value. Such quenches can be experimentally performed by tuning suitable laser intensities¹². Our prediction regarding post-quench dynamics of $O_d^{(3)}(t)$ is as follows. Below $\lambda_0 = \lambda_{0c}$, $O_d^{(3)}(t)$ will decay to zero with a characteristic timescale τ signifying the ergodic phase. The value of τ will diverge at λ_{0c} . For $\lambda_0 > \lambda_{0c}$, $O_d^{(3)}(t)$ will remain close to its original value for $t \gg \tau(\lambda_0)$. We note that $O_3^{(d)}(t)$ can be easily obtained for the present model via measurement of $\langle \hat{n}_j \rangle$. In earlier experiments, this was achieved by measuring parity of occupation of the Rydberg atoms^{6,12}.

Our proposal provides an estimate on the lower bound of timescale over which $O_d^{(3)}(t)$ needs to remain finite for claiming experimental realization of the MBL phase. The lifetime of a Rydberg chain is primarily determined by atom loss from the trap and is typically around $10\mu\text{s}$ for realistic experimental parameters¹². From Fig. 3(d), we find that the maximal decay time in the ergodic phase near the transition is $\tau_{\text{max}} \simeq 4\hbar/w \equiv 4\hbar/\Omega$. Thus for $\Omega = 4\pi\text{MHz}$, one needs to follow the dynamics for $T \gg \tau_{\text{max}} \simeq 0.3\mu\text{s}$. This requirement can be met since typical experimental timescale $t_{\text{expt}} \sim 7\mu\text{s} \simeq 22\tau_{\text{max}}$ ¹². From

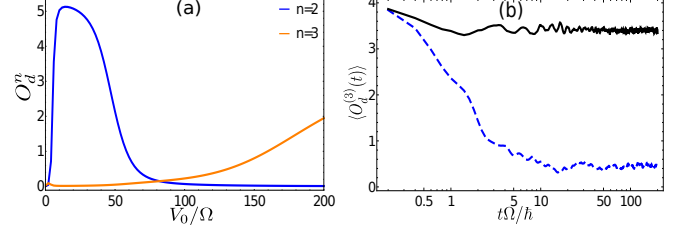


FIG. 4: (a) A plot of ground state value of the Z_2 and Z_3 order parameters as a function of V_0/Ω for a $L = 12$ Rydberg chain. We have chosen $\Delta_0/\Omega = -3$. (b) Plot of $O_d^{(3)}$ in the ergodic ($\lambda_0/\Omega = 0.5$) and MBL ($\lambda_0/\Omega = 10$) phases for $V_0/\Omega = 40$, $\Delta_0/\Omega = -3$.

Fig. 3, we indeed find that $O_d^{(3)}(t)$ decays close to zero for $t \simeq 10\tau_{\text{max}} = 40\hbar/w \simeq 3\mu\text{s}$ in the ergodic phase while it retains a finite value after this time in the MBL phase.

Finally, we provide explicit numerical evidence for signature of the MBL phase in the Rydberg atom chain using ED. An estimate of V_0 may be obtained from an ED study of the ground state H_{Ryd} for $L = 12$. We find that for $\Delta_0/\Omega = -3$ the Z_2 symmetry broken order occurs for $V_0/\Omega \leq 80$ (Fig. 4). Next we turn on the AA potential λ_j and study the response of the dipole order parameter $O_d^{(3)}$ for the Rydberg atoms. We note that the present system does not appear to exhibit a mobility edge; all states are either ergodic or localized depending on the value of λ_0 . We also find that $O_d^{(3)}$ exhibits ergodic(MBL) behavior for small (large) λ_0 (Fig. 4). The value of λ_{0c} and the period of oscillation of $O_d^{(3)}$ in the ergodic phase is found to approach those obtained from analysis H_d with increasing V_0 as expected. We thus conclude that a choice of large V_0 which is well within acceptable experimental parameter range would allow one to study the MBL phase of H_d using H_{Ryd} .

In conclusion, we have obtained the phase diagram and demonstrated the existence of an ergodic-MBL quantum phase transition for a dipole boson model in the presence of the AA potential. We have also shown that the non-equilibrium dynamics model picks up signatures of the MBL phase of this model, discussed the relevant timescales involved, and suggested concrete experiments using Rydberg atom chains which can test our theory.

Acknowledgement: A.D. acknowledges funding from SERB NPDF research grant PDF/2016/001482. SM acknowledges funding from the UGC through the Indo-Israeli project.

Appendix A: Supplemental Material for Many-body localized phase of bosonic dipoles in a tilted optical lattice

1. Ground state phase diagram

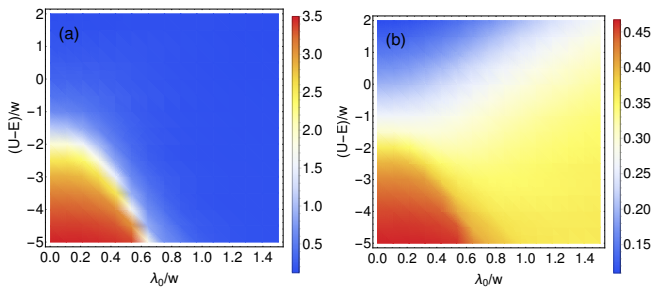


FIG. 5: (a) Phase diagram of the dipole model with AA potential showing the plot of the dipole order parameter $O_d^{(2)}$ as a function of $(U - \mathcal{E})/w$ and λ_0/w for $L = 18$. (b) The dipole density n^d as a function of $(U - \mathcal{E})/w$ and λ_0/w .

The ground state phase diagram of the model, as obtained by ED for $L = 18$ is shown in Fig. 5(a). To chart out the phase diagram, we plot the dipole order parameter $O_d^{(2)}$ in the Z_2 symmetry broken phase as a function of $(U - \mathcal{E})/w$ and λ_0/w . As expected, we find that for any given \mathcal{E} , an increase in λ_0 decreases the magnitude of $O_d^{(2)}$ and eventually the ordered phase is destroyed via a melting transition to a disordered phase. Similarly, for any given λ_0 , increasing \mathcal{E} increases the tendency towards an ordered phase. We note here that the presence of the AA potential may either aid or hinder dipole formation on a given link depending on the value of $\sin(2\pi\beta\ell)$. This can be clearly seen from Fig. 5(b) where $n^d = \langle \sum_\ell \hat{n}_\ell^d \rangle / L$ is plotted as a function of λ_0/w and $(U - \mathcal{E})/w$ showing an increase of n_d with increasing λ_0 for any \mathcal{E} . However, $O_d^{(2)}$ always decreases with increasing λ_0 .

2. Growth of the entanglement entropy in dynamics

In the main text, we showed that the entanglement entropy S allows us to distinguish between the many-body localized phase and the ergodic phase. The growth of entanglement following a quench is also a key notion in understanding the ergodic-MBL transition. The entanglement entropy following a quench grows linearly in time in the ergodic phase. In contrast, its growth is logarithmic in the MBL phase. In both cases, the entanglement entropy eventually saturates to a value, that scales with system

size L .

To study the behavior of S , we follow the same quench protocol as in the main text. We evaluate the half-chain entanglement entropy (with subsystem size $L/2$, where L is the chain length) as a function of time. The result is plotted in Fig. 6. In the ergodic regime, as shown in Fig. 6, $S(t)$ grows linearly and saturates to a value proportional to the system size L . The inset shows the system size dependence of entanglement entropy in the ergodic phase. In contrast, in the MBL phase, the growth logarithmic in time while close to the critical point the growth is faster than that inside the MBL phase. As we increase λ , we clearly find a transition from linear to logarithmic behavior marking a transition (crossover for finite size) from an ergodic to an MBL phase. We find that S is independent of the system size in the MBL phase while its L dependence in the ergodic phase is shown in the inset of Fig. 6.

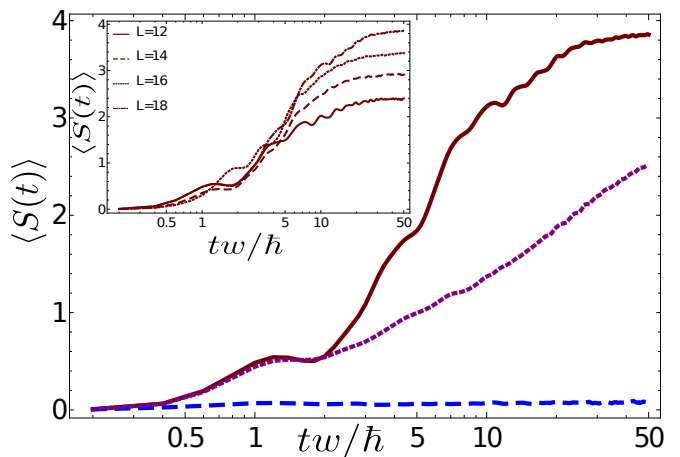


FIG. 6: The entanglement entropy after a quench with time for system size $L = 18$. The brown line is for a quench to the ergodic phase with $\delta\lambda/w = 0.5$. The blue line for a quench to the MBL phase with $\delta\lambda/w = 20$. The purple lines are for quench close to the critical point with $\delta\lambda/w = 3.095$. The inset shows value at saturation depends on the system size.

3. Bosonic dipoles in disordered and tilted optical lattice

The 1D dipole Hamiltonian we consider in Eq. 3 of the main text undergoes an ergodic-MBL transition upon varying the strength of the quasiperiodic potential λ_0 . However, the more standard setting in which MBL is observed involves the presence of quenched disorder and not a quasiperiodic potential. Here we show that the constrained dipole model in the presence of quenched

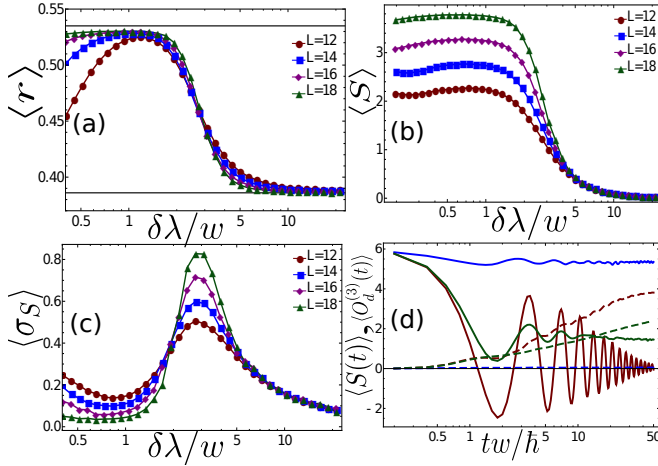


FIG. 7: (a) $\langle r \rangle$ as a function of $\delta\lambda$ showing an ergodic-MBL transition at 3.095. (b) The half-chain entanglement entropy $\langle S \rangle$ with $\delta\lambda$. (c) The fluctuation of entanglement entropy σ_S with $\delta\lambda$. (d) Plot of $\langle O_d^{(3)}(t) \rangle$ (solid lines) and entanglement entropy (dashed lines) after a quench as a function of time for system size $L = 18$. The red line is for a quench to the ergodic phase, blue for a quench to the MBL phase and green for a quench close to the ergodic-MBL critical point.

disorder also undergoes an ergodic-MBL transition. We begin by, switching off the quasiperiodic potential by setting λ_0 to zero, in the dipole Hamiltonian, Eq. (3) and instead introducing an on-site disorder potential term,

$$H_d = \sum_{\ell} (-w(d_{\ell}^{\dagger} + d_{\ell}) + \mu_d(\ell)\hat{n}_{\ell}^d) \quad n_{\ell}^d \leq 1, \quad n_{\ell}^d n_{\ell+1}^d = 0 \quad (\text{A1})$$

where $\hat{n}_{\ell}^d = d_{\ell}^{\dagger}d_{\ell}$ is the dipole number operator and

$$\mu_d(\ell) = \mu_0(\ell) + \delta\mu_{\ell} \quad (\text{A2})$$

where $\mu_0(\ell) = U - \mathcal{E}$ and $\delta\mu_{\ell}$ are independent random variables drawn from a uniform distribution $[-\delta\lambda, \delta\lambda]$. When $\delta\lambda = 0$, the model reduces to the dipole model studied earlier and in the presence of weak disorder the Hamiltonian is ergodic⁷. At a finite critical disorder strength, we show the system displays an ergodic-MBL transition. We use the same quantities discussed in the main text to understand the transition. The results obtained are shown in Fig. 7. First we plot in Fig. 7(a) the difference of the successive gaps in the energy spectrum with the strength of the disorder which shows a transition from ergodic to MBL around the critical value of $\delta\lambda_c/w = 3.09$. In Fig. 7(b) we compute the entanglement entropy for a typical state at finite energy density in the middle of the spectrum as a function of the strength of the disorder, which also shows a transition from the ergodic to MBL phase. We have also computed the fluctuations in entanglement entropy which too indicates a transition from the ergodic to MBL phase with large fluctuations at the critical point. Finally in Fig. 7 we study the nonequilibrium dynamics of the system with the same protocol discussed in the main text. We have plotted the order parameter $\langle O_d^{(3)}(t) \rangle$ (solid line) and entanglement entropy (dashed line) of the time evolved state for system size $L = 18$ for three different regimes. The red line for a quench to the ergodic phase, the blue line for a quench to the MBL phase and the green line for a quench close to critical point. In the ergodic phase, the order parameter decays to zero and entanglement entropy grows linearly to a saturation value proportional to system size L over a short time scale. In the MBL phase, the order parameter remains close to the initial value and the entanglement entropy increases very slowly (logarithmically) in time. Close to the critical point the order parameter decays slowly and the entanglement entropy grows slowly compared to ergodic phase.

- ¹ M. Greiner, O. Mandel, T. Esslinger, T.W. Hansch, and I. Bloch, *Nature (London)* **415**, 39 (2002); C. Orzel, A. K. Tuchman, M. L. Fenselau, M. Yasuda, and M. A. Kasevich, *Science* **291**, 2386 (2001).
- ² I. Bloch, J. Dalibard, and W. Zwerger, *Rev. Mod. Phys.* **80**, 885 (2008).
- ³ D. Jaksch, C. Bruder, J. I. Cirac, C. W. Gardiner, and P. Zoller, *Phys. Rev. Lett.* **81**, 3108 (1998).
- ⁴ M. P. A. Fisher, P. B. Weichman, G. Grinstein, and D. S. Fisher, *Phys. Rev. B* **40**, 546 (1989); [5] R. Pandit, K. Seshadri, H. R. Krishnamurthy, and T. V. Ramakrishnan, *Europhys. Lett.* **22**, 257 (1993).
- ⁵ K. Sengupta and N. Dupuis, *Phys. Rev. A* **71**, 033629

- (2005); J. K. Freericks, H. R. Krishnamurthy, Y. Kato, N. Kawashima, and N. Trivedi, *Phys. Rev. A* **79**, 053631 (2009); C. Trefzger and K. Sengupta, *Phys. Rev. Lett.* **106**, 095702 (2011).
- ⁶ J. Simon, W. S. Bakr, R. Ma, M. E. Tai, P. M. Preiss, and M. Greiner, *Nature (London)* **472**, 307 (2011); W. Bakr, A. Peng, E. Tai, R. Ma, J. Simon, J. Gillen, S. Foelling, L. Pollet, and M. Greiner, *Science* **329**, 547 (2010).
- ⁷ S. Sachdev, K. Sengupta, and S. M. Girvin, *Phys. Rev. B* **66**, 075128 (2002).
- ⁸ S. Pielawa, T. Kitagawa, E. Berg, and S. Sachdev, *Phys. Rev. B* **83**, 205135 (2011).
- ⁹ M. Kolodrubetz, D. Pekker, B. K. Clark, and K. Sengupta,

- Phys. Rev. B **85**, 100505 (2012).
- ¹⁰ U. Divakaran and K. Sengupta, Phys. Rev. B **90**, 184303 (2014); S. Kar, B. Mukherjee, and K. Sengupta, Phys. Rev. B **94**, 075130 (2016).
 - ¹¹ P. Fendley, K. Sengupta, and S. Sachdev, Phys. Rev. B **69**, 075106 (2004); R. Samajdar, S. Choi, H. Pichler, M. D. Lukin, and S. Sachdev, arXiv:1806.01867 (unpublished).
 - ¹² H. Bernien, S. Schwartz, A. Keesling, H. Levine, A. Omran, H. Pichler, S. Choi, A. S. Zibrov, M. Endres, M. Greiner, V. Vuletic, and M. D. Lukin, Nature **551**, 579 (2017).
 - ¹³ R. Nandkishore and D. A. Huse, Ann. Rev. Cond. Mat. Phys. **6**, 15 (2015); E. Altman and R. Vosk, Annual Review of Condensed Matter Physics **6**, 383 (2015).
 - ¹⁴ D-L Deng, S. Ganeshan, X. Li R. Modak, S. Mukerjee, and J. H. Pixley, Ann. Phys. **529**, 1600399 (2017).
 - ¹⁵ D. M. Basko, I. L. Aleiner, B. L. Altshuler, Ann. Phys. **321**, 1126-1205 (2006); V. Oganesyan and D. A. Huse, Phys. Rev. B **75**, 155111 (2007); A. Pal and D. A. Huse, Phys. Rev. B **82**, 174411 (2010); D. A. Huse, R. Nandkishore, V. Oganesyan, A. Pal, and S. L. Sondhi, Phys. Rev. B **88**, 014206 (2013); R. Vosk, E. Altman, Phys. Rev. Lett. **110**, 067204 (2013); M. Serbyn, Z. Papic, D. A. Abanin, Phys. Rev. Lett. **111**, 127201 (2013); D. A. Huse, R. Nandkishore, V. Oganesyan, Phys. Rev. B **90**, 174202 (2014); T. Grover, arXiv:1405.1471 (unpublished); M. Serbyn, Z. Papic, and D. A. Abanin, Phys. Rev. X **5**, 041047 (2015); K. Agarwal, S. Gopalakrishnan, M. Knap, M. Mueller, and E. Demler, Phys. Rev. Lett. **114**, 160401 (2015); V. Khemani, S. P. Lim, D. N. Sheng, and D. A. Huse, Phys. Rev. X **7**, 021013 (2017).
 - ¹⁶ J. H. Bardarson, F. Pollmann, J. E. Moore, Phys. Rev. Lett. **109**, 017202 (2012); S. Iyer, V. Oganesyan, G. Refael, and D. A. Huse, Phys. Rev. B **87**, 134202 (2013); J. A. Kjall, J. H. Bardarson, and F. Pollmann, Phys. Rev. Lett. **113**, 107204 (2014); R. Vasseur, S. A. Parameswaran, J. E. Moore, Phys. Rev. B **91**, 140202 (2015); M. Serbyn, Z. Papic, D. A. Abanin, Phys. Rev. B **90**, 174302 (2014); D. Pekker, G. Refael, E. Altman, E. Demler, and V. Oganesyan, Phys. Rev. X **4**, 011052 (2014); R. Modak and S. Mukerjee, Phys. Rev. Lett. **115**, 230401 (2015); D. J. Luitz, N. Laflorencie, and F. Alet, Phys. Rev. B **91**, 081103 (2015); W. De Roeck, F. Huveneers, M. Mueller, and M. Schiulaz, Phys. Rev. B **93**, 014203 (2016); R. Modak, S. Ghosh and S. Mukerjee, Phys. Rev. B **97**, 104204 (2018).
 - ¹⁷ M. Schreiber, S. S. Hodgman, P. Bordia, H. P. Luschen, M. H. Fischer, R. Vosk, E. Altman, U. Schneider and I. Bloch, Science **349**, 842 (2015).
 - ¹⁸ J. Smith, A. Lee, P. Richerme, B. Neyenhuis, P. W. Hessel, P. Hauke, M. Heyl, D. A. Huse, and C. Monroe, Nat. Phys. **12**, 907 (2016).
 - ¹⁹ See Supplemental Material for details.
 - ²⁰ P. Naldesi, E. Ercolessi, and T. Roscilde, SciPost Phys. **1**, 010 (2016).
 - ²¹ R. Ghosh, A. Sen, and K. Sengupta, Phys. Rev. B **97**, 014309 (2018).
 - ²² K Singh, K Saha, S. A Parameswaran, and D. M Weld, Phys. Rev. A **92**, 063426 (2015).